Cell Death and Differentiation (2006) 13, 426–434

www.nature.com/cdd

CED-4 forms a 2 : 2 heterotetrameric complex with CED-9 until specifically displaced by EGL-1 or CED-13

WD Fairlie*[,1], MA Perugini[2,3], M Kvansakul[1], L Chen[1], DCS Huang[1] and PM Colman[1]

[1] The Walter and Eliza Hall Institute of Medical Research, Parkville, Victoria, Australia
[2] Russell Grimwade School of Biochemistry and Molecular Biology, University of Melbourne, Parkville, Victoria, Australia
[3] Bio21 Molecular Science and Biotechnology Institute, University of Melbourne, Parkville, Victoria, Australia
* Corresponding author: WD Fairlie, Structural Biology Division, The Walter and Eliza Hall Institute of Medical Research, 1G Royal Parade, Parkville, Victoria 3050, Australia. Tel: +61 3 9345 2309; Fax: +61 3 9345 2686; E-mail: fairlie@wehi.edu.au

Received 22.3.05; revised 29.7.05; accepted 03.8.05; published online 16.9.05
Edited by M Hengartner

Abstract

The pathway to cell death in *Caenorhabditis elegans* is well established. In cells undergoing apoptosis, the Bcl-2 homology domain 3 (BH3)-only protein EGL-1 binds to CED-9 at the mitochondrial membrane to cause the release of CED-4, which oligomerises and facilitates the activation of the caspase CED-3. However, despite many studies, the biophysical features of the CED-4/CED-9 complex have not been fully characterised. Here, we report the purification of a soluble and stable 2 : 2 heterotetrameric complex formed by recombinant CED-4 and CED-9 coexpressed in bacteria. Consistent with previous studies, synthetic peptides corresponding to the BH3 domains of worm BH3-only proteins (EGL-1, CED-13) dissociate CED-4 from CED-9, but not from the gain-of-function CED-9 (G169E) mutant. Surprisingly, the ability of worm BH3 domains to dissociate CED-4 was specific since mammalian BH3-only proteins could not do so.
Cell Death and Differentiation (2006) **13,** 426–434.
doi:10.1038/sj.cdd.4401762; published online 16 September 2005

Keywords: apoptosis; *Caenorhabditis elegans*; CED-4; CED-9; EGL-1; Bcl-2; APAF-1

Abbreviations: Bcl-2, B-cell lymphoma-2; BH3, Bcl-2 homology domain 3; CARD, caspase recruitment domain; NB-ARC, nucleotide-binding domain shared by APAF-1, certain *R* gene products and CED-4; ITC, isothermal titration calorimetry; APAF-1, apoptotic protease-activating factor 1

Introduction

Much of our current understanding of the pathways to programmed cell death has been learned from genetic analysis of the nematode *Caenorhabitditis elegans*.[1] In this organism, three genes essential for the execution of apoptosis have been identified, namely *ced-3*, *ced-4*,[2] and *egl-1*,[3] whereas another, *ced-9*, antagonizes cell death.[4] In healthy cells, the adapter CED-4 associates with CED-9, the worm B-cell lymphoma-2 (Bcl-2) orthologue, on mitochondrial membranes.[5] When the cell receives a death signal, transcriptionally upregulated Bcl-2 homology domain 3 (BH3)-only protein EGL-1 binds CED-9. This, in turn, releases CED-4 allowing its oligomerisation and leads to the activation of the caspase CED-3 which is synthesised as an inactive zymogen.[6] CED-4 facilitates proteolytic autoactivation of CED-3 by bringing CED-3 zymogens into close proximity through interactions between their caspase-recruitment domains (CARDs) (Figure 1). However, it is not known whether the CED-4/CED-9 complex at the mitochondrial membrane contains CED-3 constitutively, although during cell death, CED-4 dissociates from CED-9 and translocates from the mitochondrial to the nuclear membrane.[5]

This pathway of protein interactions has been extensively studied using a myriad of techniques. For example, interaction of CED-4 with CED-9 (and simultaneously with CED-3) has been demonstrated by co-immunoprecipitation of proteins expressed in various cell types,[6–8] the yeast two-hybrid system,[9–11] or by colocalization studies.[5,12,13] These have been complemented by mutational analysis of both CED-4 and CED-9.[9,10,14] Similarly, numerous studies have demonstrated the interaction between CED-9 and EGL-1, and release and/or redistribution of CED-4 from the mitochondria.[3,12,14–16]

Recently, three-dimensional structures were determined for the Bcl-2 homology region of CED-9 alone,[16] and in complex with an EGL-1 fragment encompassing its BH3 domain,[14] confirming the structural similarity with the mammalian Bcl-2 prosurvival family members[17,18] and their mode of engagement with BH3 domains.[19–21] These structures of CED-9 suggest a mechanism by which CED-4 is released from CED-9. Binding of EGL-1 through its BH3 domain to a hydrophobic cleft in CED-9 results in a substantial structural rearrangement in CED-9, which is proposed to disrupt binding to CED-4 at a second site on CED-9.[14] The CED-9/EGL-1 complex structure also explained a *ced-9* gain-of-function mutation that prevents most somatic cell deaths in *C. elegans*.[22] This mutation substitutes the highly conserved glycine residue at position 169 with glutamic acid and prevents EGL-1-induced release of CED-4, but preserves CED-4 binding to CED-9.[5,8,15] The CED-9/EGL-1 complex structure shows that the replacement of glycine with glutamic acid would introduce a steric clash with EGL-1, thereby negatively affecting its binding.[14]

The three-dimensional structure of the mammalian homologue of CED-4, apoptotic protease-activating factor 1 (APAF-1), with WD40 domains deleted, has also recently been solved.[23] This structure showed a relatively compact protein of five distinct domains with the amino terminal CARD at one end and the C-terminus at the other (Figure 1). An ADP molecule was found deeply buried within the protein at the junction of four domains and appears to serve as an organising centre to

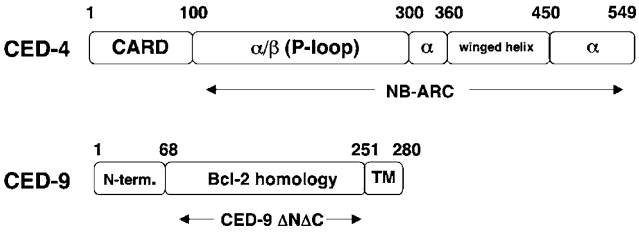

Figure 1 Domain architecture of CED-4 and CED-9. CED-4 consists of an N-terminal caspase recruitment domain (CARD) required for binding CED-3 and a C-terminal nucleotide-binding domain shared by APAF-1, certain plant *R* gene products and CED-4 (NB-ARC). The subdomain structure shown is taken from the APAF-1 structure.[23] CED-9 has an N-terminal domain, a central domain homologous to mammalian Bcl-2 prosurvival proteins, and a C-terminal hydrophobic transmembrane segment that was deleted in all constructs used

lock the molecule into an inactive state. Owing to the packing of the CED-4 CARD in this structure, a conformational change, presumably as a consequence of ATP hydrolysis, is required for interaction with the caspase-9 prodomain.

Most of the above functional studies on the CED-3/CED-4/CED-9 interaction and its modulation by EGL-1 have been done in cell-based assays, and have thus not addressed relevant biophysical questions regarding these macromolecular complexes, although some attempts at characterising recombinant proteins have been reported. For example, it has been shown that recombinant CED-4 produced in insect cells spontaneously oligomerises,[24] a result consistent with studies indicating that CED-9 prevents CED-4 oligomerisation.[6] Gel-filtration chromatography estimates of the mass of the CED-4 oligomers produced from the various constructs used in this study ranged from 500 to 1500 kDa. However, no studies to date have addressed the question of the size and stoichiometry of the CED-9/CED-4 complex. In this paper we report, for the first time, high-level expression of recombinant CED-4/CED-9 complex in bacteria. This purified protein complex is a 2 : 2 heterotetramer and responds predictably to treatment with EGL-1. Furthermore, we demonstrate that the trigger required for release of CED-9 from CED-4 is highly specific since it can only be initiated by worm, but not mammalian, BH3-only proteins.

Results

Expression and purification of CED-4/CED-9 complex

To study the biochemical properties of the adapter molecule CED-4, we initially attempted to express either the full-length protein or its predicted domains in *Escherichia coli*. These fragments included the N-terminal CARD, the nucleotide-binding domain shared by APAF-1, certain *R* gene products and CED-4 (NB-ARC) or a shorter form of the NB-ARC that just encompassed the P-loop ATP-binding domain (Figure 1). In all cases, relatively high levels of protein were expressed (mg/l of culture) but their poor solubility precluded us from purifying and characterising them in detail.

To circumvent this problem, we attempted coexpressing CED-4 with its physiological binding partner, CED-9,[9] using a dual expression vector. Although most of the CED-4

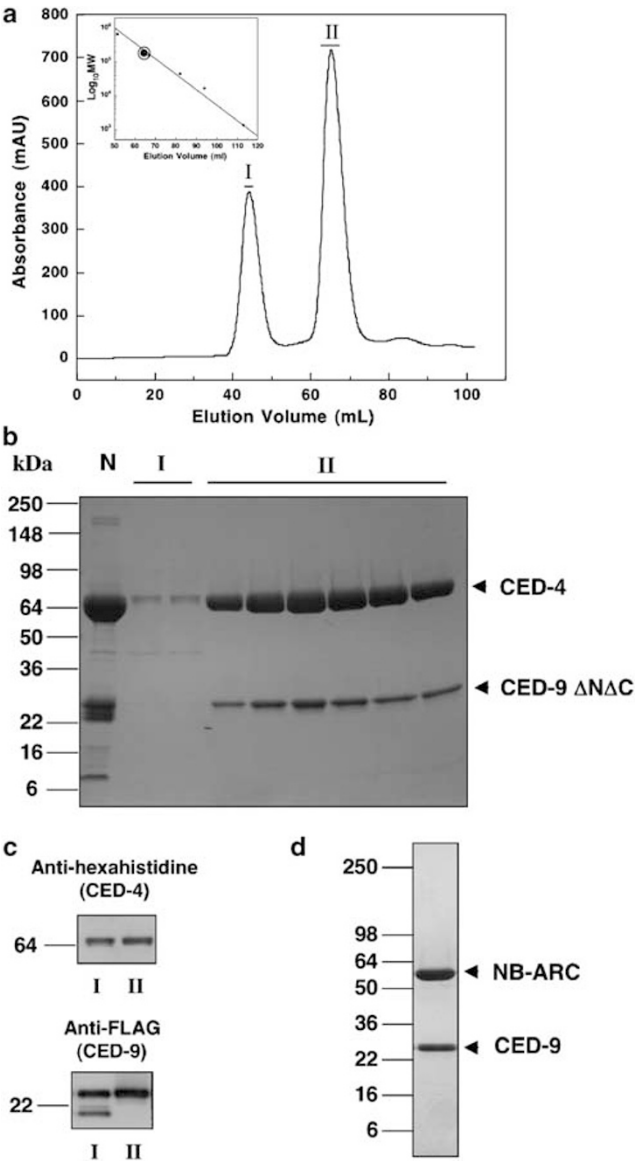

Figure 2 Purification of CED-4/CED-9 complex. (**a**) Gel-filtration profile of CED-4/CED-9 complex following Nickel-affinity chromatography. The inset shows a standard curve based on the retention time of molecular weight standards. The circled point indicates the apparent molecular weight/retention time of the protein complex in Peak II. (**b**) Coomassie Blue-stained gel of the eluate from Nickel-affinity chromatography (N), or fractions from Peak I and II of CED-4/CED-9 complex purified as indicated in (**a**). (**c**) Western blot analysis of the central fractions from Peaks I or II isolated in (**a**). Hexahistidine-tagged CED-4 and FLAG-tagged CED-9 are present in both peaks. (**d**) Coomassie Blue-stained gel of the main fraction of purified CED-4 NB-ARC/CED-9 complex

expressed using this system remained insoluble, there was sufficient soluble material to allow purification of a complex of CED-4 with CED-9. Encouragingly, 1–10 mg (per litre of bacterial culture) of the protein complex was isolated from the soluble fraction of bacterial lysates using a two-step purification protocol involving an initial Nickel-affinity purification step (employing the hexahistidine tag on the N-terminus of CED-4) followed by a gel-filtration chromatography step (Figure 2a–c). Typically, the gel-filtration chromatogram

of protein complexes recovered from the Nickel-affinity purification indicated that, in some preparations, up to one-third of the purified material was a soluble high molecular weight aggregate, which eluted near the column void volume (Figure 2a, Peak I). Western blot analysis of this peak showed that it, like the major peak (Figure 2a, Peak II), contained both CED-4 and CED-9, although unlike the major peak it includes a putative CED-9 degradation product (Figure 2c). The Peak I complex also displayed a relatively high absorbance at 340 nm, suggesting that it may be a soluble protein aggregate. Therefore, subsequent studies used only the major fraction eluted in Peak II (Figure 2a).

We tested two different CED-9 constructs in the coexpression studies: one lacking its C-terminal hydrophobic tail (CED-9ΔC) and another in which both the hydrophobic tail and the amino-terminal 67 residues were removed (CED-9ΔNΔC) (Figure 1). The gel-filtration profiles of the complex containing either of these CED-9 constructs were very similar (data not shown). As the CED-9ΔNΔC protein expressed alone was generally more soluble, and thus more readily amenable for further characterisation, we focused our efforts on complexes formed between this protein and CED-4. In fact, purified CED-4/CED-9ΔNΔC complex could be concentrated to reasonably high levels (>30 mg/ml) without further aggregation apparent, as judged by re-chromatography on a size-exclusion column. This complex was also stable after up to 2 weeks storage at 4°C with the appearance of only a minor peak (less than 20% of total protein) corresponding to the CED-9ΔNΔC protein in the size-exclusion profile upon rechromatography (data not shown).

We were similarly able to express and purify a complex of the NB-ARC/CED-9ΔNΔC, indicating that the CARD of CED-4 is dispensable for binding to CED-9 (Figure 2d) This is consistent with previous reports.[10] Interestingly, deletion of just five residues from the C-terminus of CED-4, however, prevented production of soluble complex.

Stoichiometry of the CED-4/CED-9ΔNΔC complex

Coomassie Blue staining of the CED-4/CED-9ΔNΔC complex (Peak II in Figure 2a) on SDS-PAGE gels suggested that the ratio of CED-4 to CED-9ΔNΔC may be greater than 1 : 1, as the CED-4 band appeared significantly more intense (Figure 2b). This was the case whether the complex was isolated using the Nickel-affinity column alone, or in conjunction with gel-filtration chromatography.

To perform a more quantitative analysis of the stoichiometry of the protein complex, it was subjected to six cycles of amino-terminal sequencing. Accurate values for amino-acid abundance on each cycle could be readily obtained for all amino acids except aspartates due to technical limitations. The ratio of abundance of CED-9 residues to CED-4 residues was very close to a stoichiometric 1 : 1 ratio (Table 1). This suggests that the staining pattern observed on the SDS-PAGE gel may be due to preferential staining of CED-4 or poor staining of CED-9. Such anomalous staining has been reported for other proteins, such as certain surface proteins of *Candida albicans*.[25]

Size and solution properties of the CED-4/CED-9ΔNΔC complex

The majority of the purified protein complex in more than 10 different preparations eluted at a retention time (Peak II, Figure 2a) on gel-filtration consistent with a complex of approximately 180–200 kDa. This mass estimate, determined from calibration curves on several different columns (e.g. see inset, Figure 2a), together with the stoichiometry data (Table 1), suggested that the complex might be a hetero-tetramer consisting of two molecules each of CED-4 and CED-9ΔNΔC, for which the calculated mass is 175 kDa. The apparent size on gel filtration was the same regardless of whether the FLAG tag was present at the amino terminus of the CED-9ΔNΔC, indicating that artificial dimerisation through the FLAG tag was not responsible for the formation of the complex (data not shown).

To get a more accurate assessment of the size of the complex, analytical ultracentrifugation was performed. Sedimentation velocity studies of the complex were initially conducted in Tris-buffered solution at a total protein concentration of 1.0 mg/ml. The absorbance *versus* radial position profiles are plotted at 6 min intervals in Supplementary Figure 1b. Continuous size-distribution analysis of this data yields an excellent fit to a predominantly single species with a sedimentation coefficient ($s_{20,w}$) of 7.5 S (Supplementary Figure 1c), an apparent molar mass of 159 kDa and frictional ratio of 1.40. This suggests that the CED-4/CED-9ΔNΔC complex may exist as either a 2 : 1 or 2 : 2 CED-4/CED-9ΔNΔC complex. Therefore, to confirm the quaternary structure of the CED-4/CED-9ΔNΔC complex, sedimentation equilibrium experiments, which are independent of molecular shape estimates and therefore give a more robust measure of molecular mass,[26] were also conducted at an initial protein concentration of 1.0 mg/ml (Supplementary Figure 1d–f). The nonlinear least-squares best-fit yielded a molar mass of 180 ± 3.8 kDa, in excellent agreement with the theoretical heterotetrameric mass of a 2 : 2 CED-4/CED-9ΔNΔC complex (175 kDa).

Table 1 Amino terminal sequencing of the CED-4/CED-9 complex

Cycle	1	3	5	6
CED-4 residue (yield) (pmol)	Gly (10.4)	His (5.7)	His (9.4)	His (8.3)
CED-9 residue (yield) (pmol)	Ala (10.2)	Leu (4.5)	Tyr (9.3)	Lys (5.7)

Amino acid yields on each sequencing cycle are presented except for cycles 2 and 4 where aberrantly high yields of aspartic acid present in CED-9 was obtained. The sequences are those of the tagged recombinant proteins rather than their native counterparts in which the amino terminal six residues of hexahistidine-tagged CED-4 is GSHHHH and of FLAG-tagged CED-9 is ADLDYK

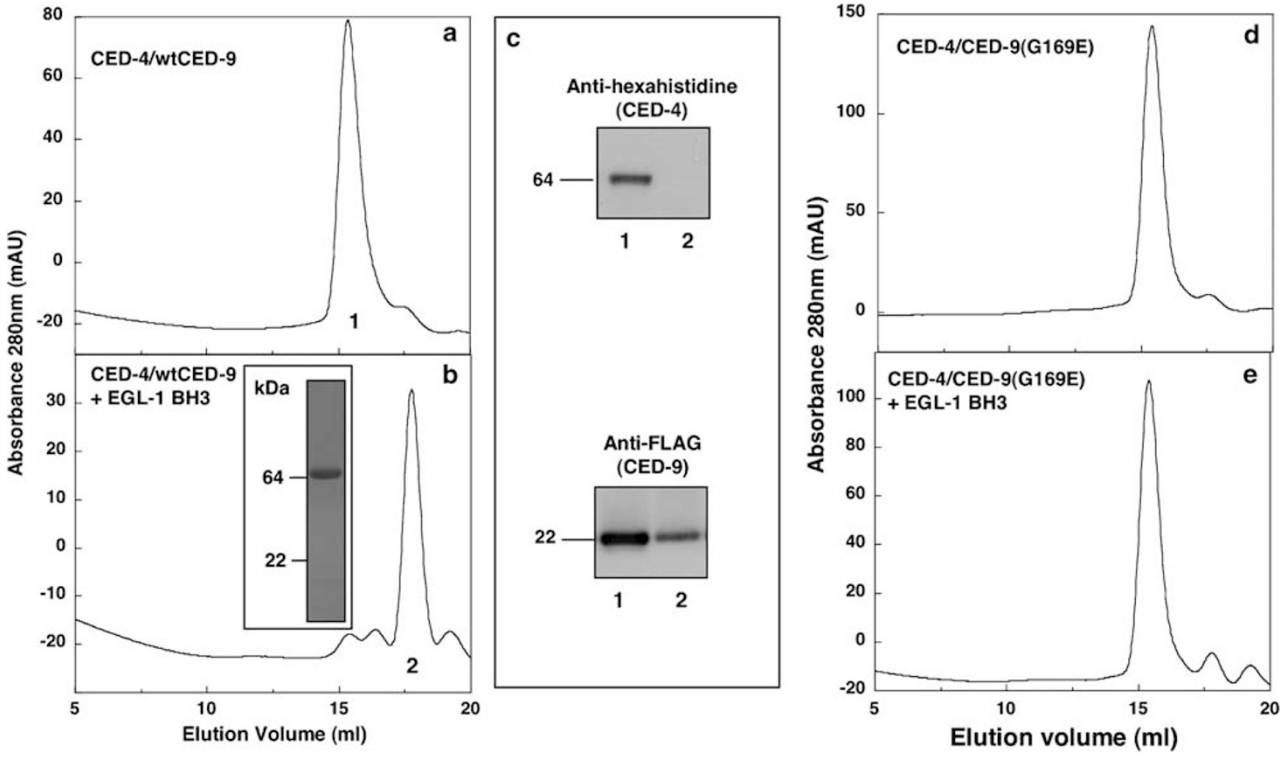

Figure 3 EGL-1 BH3 domain-induced dissociation of CED-4/CED-9 complex. CED-4 in complex with wild-type CED-9 (**a, b**) or a gain-of-function mutant CED-9 (G169E) (**d, e**) was incubated alone (**a, d**) or in the presence of a synthetic peptide spanning the EGL-1 BH3 (**b, e**) before gel-filtration chromatography. Note the shift of the retention position of Peak 1 in (**a**) to a smaller sized protein in Peak 2 in (**b**). The inset in (**b**) shows a Commasie-stained gel of the insoluble protein removed prior to chromatography. Only protein of the size of CED-4 was present. (**c**) The identity of the proteins in the two major peaks was confirmed by Western blot analysis. Peak 1 contains both the hexahistidine-tagged CED-4 and FLAG-tagged CED-9 proteins, while Peak 2 contains only CED-9. (**d, e**) Addition of the EGL-1 BH3 peptide did not affect the complex formed between a gain-of-function mutant of CED9 (G169E) and CED-4

EGL-1 BH3 domain displaces CED-4 from CED-9

The current model for the apoptosis pathway in worms proposes that binding of the BH3-only protein EGL-1 to CED-9 results in displacement of bound CED-4.[3,12,15] If this is correct, we predict that the CED-4/CED-9 complex formed *in vitro* (Figure 2a, Peak II) would be disrupted by EGL-1. When the purified CED-4/CED-9ΔNΔC complex was incubated with a synthetic 26-mer peptide encompassing the BH3 domain of EGL-1, a visible precipitate formed, which was removed by centrifugation. Gel-filtration chromatography of the soluble material demonstrated dissociation of CED-4 from CED-9ΔNΔC, with essentially no protein detected where the untreated complex normally elutes (Figure 3a,b). Only a peak corresponding to an ~25 kDa protein was detected, which on Western blotting was shown to contain FLAG-tagged CED-9ΔNΔC (Figure 3c), but not CED-4. Instead, all of the CED-4 appeared to be contained in the insoluble pellet removed by centrifugation prior to chromatography (see inset, Figure 3b).

Importantly, the release of the CED-4 from the complex appeared to be dependent upon a specific interaction of the EGL-1 BH3 peptide with wild-type CED-9. A single point mutation in CED-9, substituting the highly conserved glycine at position 169 with glutamate, which has been reported to effect EGL-1 binding,[8,15] completely prevented the EGL-1 BH3 domain peptide from displacing CED-4 (Figure 3d,e). However, the ability of this mutant CED-9 to bind CED-4 was unaffected (Figure 3d), which may explain why this mutant is a more potent inhibitor of cell death[4] since it can no longer be restrained by EGL-1.

Similar results were obtained using isothermal titration microcalorimetry (Figure 4). In these studies, EGL-1 peptide was titrated into the CED-4/CED-9ΔNΔC complex. In the initial EGL-1 peptide injections into the CED-4/CED-9ΔNΔC-containing solution, heat was released (Figure 4a), indicating a binding event between the peptide and the complex. However, a pronounced baseline shift was then observed upon subsequent additions of peptide. This shift may be due to aggregation/precipitation of CED-4 released from the complex as the solution removed from the isothermal titration calorimetry (ITC) cell at the completion of the titration was noticeably turbid. SDS-PAGE analysis of the pellet postcentrifugation confirmed that it contained predominantly CED-4 (data not shown). The system is thermodynamically complex involving several potential reactions all of which release or absorb heat (i.e. EGL-1 peptide binds CED-9, CED-4 release from CED-9, CED-4 oligomerisation/precipitation), and hence quantitative analysis of the data is difficult.

However, the results provide qualitative evidence that aggregation of CED-4 occurs very soon after dissociation from CED-9 (Figure 4a). When a complex containing the CED-9ΔNΔC (G169E) was similarly analysed, no initial heat release or significant baseline shift was observed (Figure 4b) This confirms our gel-filtration results that EGL-1 BH3 could not bind mutant CED-9ΔNΔC (G169E) (Figure 3d,e).

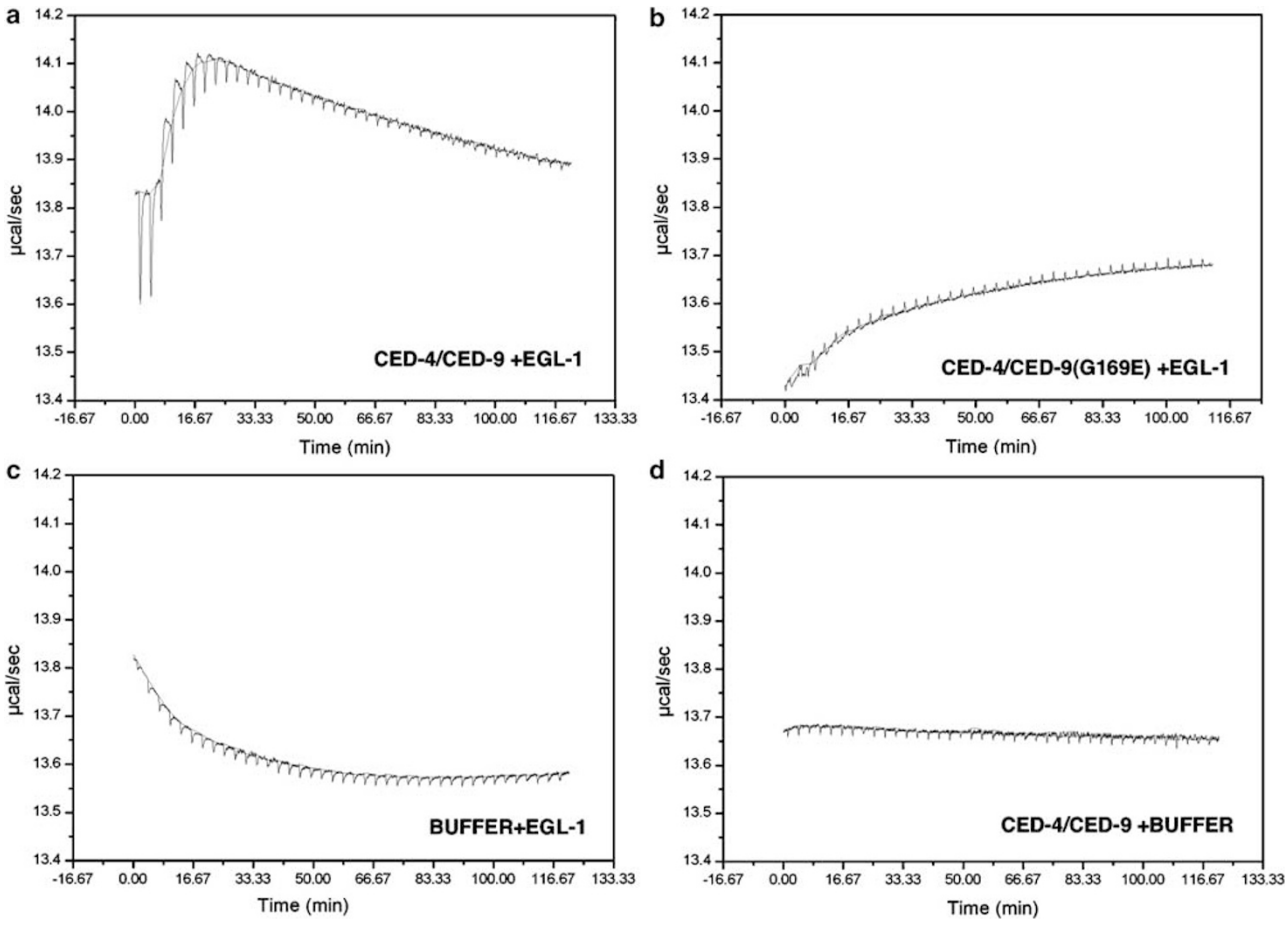

Figure 4 CED-4/CED-9 complex dissociation demonstrated by isothermal titration calorimetry (ITC). Raw data from isothermal calorimetry experiments with CED-4/CED-9 or CED-4/CED-9 (G169E) complexes. EGL-1 BH-3 peptide was titrated into solution (**a**) containing CED-4/CED-9, (**b**) CED-4/CED-9 (G169E), or (**c**) buffer only. In (**d**), buffer only was titrated into solution containing CED-4/CED-9 complex

Unlike worm BH3-only proteins, mammalian BH3-only proteins cannot disrupt the CED-4/CED-9 complex

Using isothermal titration calorimetry, we were able to directly determine the affinity of EGL-1 BH3 peptide for free (uncomplexed) CED-9ΔNΔC. The K_D for this interaction was approximately 25 nM, consistent with a previously reported value (6 nM) measured by ITC using a comparable EGL-1 peptide.[16] Recently, a second BH3-only protein, CED-13, was discovered in the worm.[27] Its BH3 domain sequence shows significant homology with that of EGL-1 (Figure 7), and over-expression of CED-13 in *C. elegans* promotes apoptosis.[27] We therefore compared the ability of CED-13 to bind CED-9 and found that the affinity of a peptide spanning this BH3 domain was approximately four-fold lower ($\sim$100 nM) than that of the EGL-1. Consistent with this, we observed that the CED-13 BH3 peptide can also disrupt the CED-4/CED-9ΔNΔC complex, but with lower efficiency as demonstrated by a significant proportion of the complex remaining after treatment (Figure 5b).

Since both worm BH3-only proteins can displace CED-4 from CED-9, the evolutionary conservation of the cell death pathways prompted us to test if mammalian BH3-only proteins can also trigger this dissociation. As mammalian Bcl-2 can function in worms,[4,28] we wondered if mammalian BH3-only proteins such as Bim, which can bind to all known mammalian prosurvival proteins, could substitute for worm EGL-1. We found instead that Bim BH3 peptide could not bind CED-9ΔNΔC in direct binding studies, using isothermal titration calorimetry (data not shown), and consistent with this, Bim BH3 peptide did not disrupt the complex formed between CED-4 and CED-9ΔNΔC (Figure 5c). Furthermore, synthetic peptides corresponding to the BH3 domain sequence from several other mammalian BH3-only proteins, Bid, Bad, Noxa or Puma, did not cause any complex dissociation (data not shown).

To determine whether complex dissociation could involve more than just the BH3 domain sequence, we examined the ability of the promiscuous-binding full-length Bim_S protein to interact with the CED-4/CED-9 complex. In an initial experiment, bacterially expressed recombinant full-length Bim_S protein was used in place of the BH3 domain peptide. This protein, as with the peptide, was unable to dissociate or interact with the purified CED-4/CED-9 complex as determined by both gel-filtration and ITC experiments (data

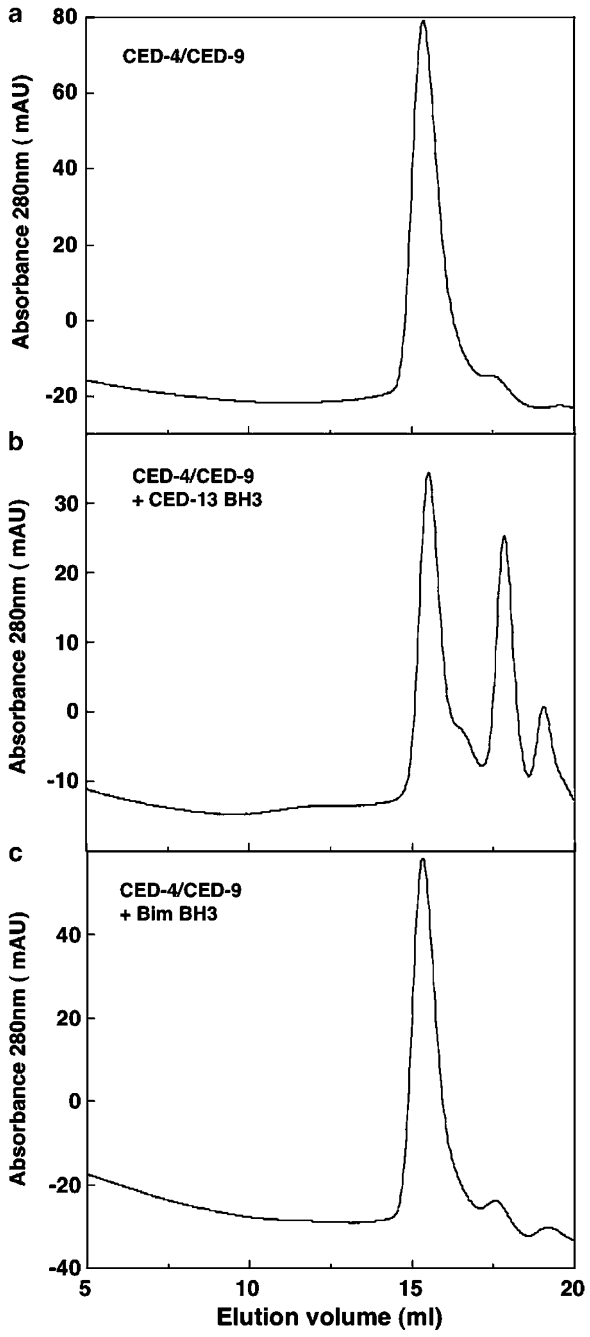

Figure 5 *C. elegans* CED-13 BH3, but not Bim BH3 dissociate CED-4 from CED-9. The purified CED-4/CED-9 complex was incubated (**a**) alone, or with synthetic peptides corresponding to (**b**) CED-13 BH3 or (**c**) Bim BH3 prior to gel-filtration chromatography. Note the partial complex dissociation with CED-13 BH3 peptide, whereas addition of Bim BH3 had no impact

not shown). This was confirmed in co-immunoprecipitation experiments (Figure 6). In these experiments, expression of EGL-1 prevented association of CED-4 with CED-9. However, consistent with studies using bacterially- expressed recombinant material, expression of Bim_s had no effect on complex formation/dissociation (Figure 6). Taken together, these binding studies confirm the selectivity of worm BH3-proteins (EGL-1 and CED-13) for CED-9.

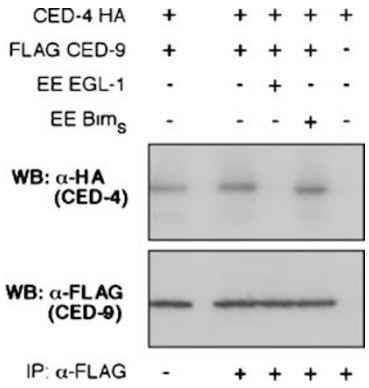

Figure 6 *C. elegans* EGL-1, but not human Bim_S, dissociate CED-4 from CED-9. Equivalent lysates prepared from 293T cells cotransfected with constructs encoding HA-tagged CED-4 and FLAG-tagged CED-9 and either EE-tagged CED-9 or EE-tagged Bim_S were immunoprecipitated with anti-FLAG antibodies and immunoblotted with both anti-HA (upper panel) or anti-FLAG (lower panel) antibodies. EGL-1 expression disrupts the CED-4/CED-9 complex, but Bim_s was unable to do so

Discussion

In *C. elegans*, the life-or-death fate of a cell is dependent upon whether the adapter protein CED-4 is sequestered by CED-9. In this manuscript we have shown for the first time that the CED-4/CED-9 complex can exist as a heterotetramer in aqueous solution, with the size and stoichiometry of the complex determined from gel-filtration chromatography (Figure 2), N-terminal sequencing (Table 1) and analytical ultracentrifugation (Supplementary Figure 1). This complex is (coexpressed) at milligram per litre quantities in *E. coli* and is highly soluble. In contrast, attempts to purify similar levels of CED-4 alone were hindered by the protein's insolubility and tendency to aggregate into inclusion bodies. Previously, the expression of soluble GST-fusions of CED-4 has been reported,[8,14,24] although the amounts of protein produced in these studies is unclear, while other attempts to coexpress CED-4 and CED-3 resulted only in the production of insoluble proteins.[29] While we cannot eliminate the possibility that the CED-4/CED-9 complex known to be associated with the mitochondrial membrane in the worm exists in a different oligomeric form to that described here for the *E. coli*-derived complex, our biochemical data for different complexes, including mutants, are consistent with the features of the protein complex characterised previously.[5,6,8–10,12,15]

For example, we have shown that the formation of the complex is not dependent on the presence of the CARD of CED-4, consistent with the requirement that it be free to recruit CED-3 to a trimolecular complex of CED-3/CED-4/CED-9.[7] This result agrees with other studies using yeast two-hybrid assays showing a strong interaction between CED-9 and CED-4 with its CARD deleted.[10] Importantly, we also demonstrated that the heterotetrameric CED-4/CED-9ΔNΔC complex dissociated upon incubation with a synthetic peptide corresponding to the BH3 domain of EGL-1 providing evidence that the complex produced here in *E. coli* behaves functionally in a manner similar to that reported in transfected cells (Figure 6)[12,15] and in worms.[5] Furthermore, we demonstrated that introduction of the G169E gain-of-function mutation into CED-9ΔNΔC prevented EGL-1 BH3 peptide-induced

Figure 7 Sequences of BH3 peptides used. The BH3 domains of the indicated BH3-only proteins were synthesised as 26-mers. Shaded residues indicate identity with the EGL-1 sequence

release of CED-4 from the complex as shown previously.[5] In addition, no binding was detected between the EGL-1 BH3 peptide and the complex involving this CED-9ΔNΔC(G169E) mutant in our ITC studies. These results agree with the previously observed failure of CED-4 to be released from the mitochondria in cells expressing this CED-9 mutant,[5] and structural studies that show that the G169E substitution occludes the BH3-binding groove.[14]

Our experiments also support observations by others that, in the absence of CED-9, CED-4 self-associates.[5,24] Using purified recombinant proteins, we have shown that following EGL-1 BH3 peptide-induced release of CED-4 from CED-9, CED-4 forms an insoluble aggregate. The ITC studies also suggest that this aggregation occurs very soon after EGL-1 BH3 peptide-induced release from CED-9. This tendency for CED-4 to aggregate/self-associate may explain why expression of high levels of soluble CED-4 in *E. coli* was not possible. However, it may be the case that this aggregation process would be less pronounced or, at least, more controlled if CED-4 were bound to CED-3, as may be the case in cells.

We also examined the ability of BH3 domains from proteins other than EGL-1 (Figure 5) to dissociate the CED-4/CED-9ΔNΔC complex. The BH3 domain sequence from another nematode protein, CED-13, was able to displace CED-4 from CED-9, although it was less effective than the EGL-1 peptide. This weaker dissociating activity was reflected in the approximately four-fold lower affinity of the peptide for CED-9. CED-13 binding to CED-9 in *C. elegans* has been reported, although the proapoptotic phenotype of CED-13 is apparently weaker than that of EGL-1.[27] The weaker affinity of CED-13 for CED-9ΔNΔC compared to that of EGL-1 may provide a partial rationale for this observation. Interestingly, BH3 domain sequences from the mammalian BH3-only proteins Bim, Puma, Noxa, Bad, and Bid were completely ineffective at dissociating the complex, consistent with the absence of binding of Bim to free CED-9ΔNΔC in our ITC studies. We have previously shown that both Bim and Puma can bind with high affinity (dissociation equilibrium constants in the low nanomolar range) to all known mammalian Bcl-2 family proteins, while Noxa, Bad and Bid have more restricted specificities.[30] Among the central 16 residues at the core of the BH3 domains illustrated in Figure 7, the EGL-1 sequence is preserved at 10 of these positions in one or more of the mammalian proteins. If the BH3 domains of all known human BH3-only proteins[30] are included in the comparison (although not all have been assayed here), the number increases to 13 (or 14 if the Cys for Ser substitution is discounted). Thus, a significant residual of the worm EGL-1 sequence persists in the BH3-only proteins in mammals, but none of those tested here can displace CED-4 from CED-9. Hence, this inability of BH3 domain sequences from mammalian BH3-only proteins to displace CED-4 further illustrates aspects of the specificity between BH3 domains and prosurvival molecules.

The observation that the CED-4/CED-9ΔNΔC complex is heterotetrameric has a number of implications. Site-directed mutagenesis studies of CED-9 indicate that residues in a surface patch adjacent to the BH3 domain-binding groove on CED-9 are involved in the interaction with CED-4;[14] however, our data suggest that a yet-to-be characterised binding surface on either or both of the components is involved in dimerisation of the CED-4/CED-9 complex. Further, our data indicate that this binding surface involves neither the membrane anchor nor the N-terminal 67 residues of CED-9. The absence of evidence for a dimer of CED-9 in solution suggests that CED-4 may mediate dimerisation of the CED-4/CED-9ΔNΔC complex. In that case, the NB-ARC would be implicated in the homodimerisation of CED-4 as the complex can be formed in the absence of the CED-4 CARD. Furthermore, our finding that deletion of just five residues from the C-terminus of CED-4 prevented production of soluble complex suggests that the interface for complex formation includes the C-terminus of CED-4. In the APAF-1 structure, the C-terminal residues are located on a short helix at the opposite end of the molecule to the N-terminus and, importantly, are quite distinct from the other four protein domains.[23] Hence, the inability to produce soluble protein with the short C-terminal deletion is unlikely due to failure of the CED-4 proteins to fold, but is more likely due to a failure in the assembly of the complex.

It is known that CED-3 can bind to the CED-4/CED-9 complex[7,31] and that activation of CED-3 occurs following displacement of CED-9 and oligomerisation of CED-4. We have shown that the heterotetramer does not depend on the presence of the N-terminal CARD of CED-4, which suggests that in this complex it is 'available' to bind its cognate CARD on CED-3. If this model holds for a ternary CED-3/CED-4/CED-9 complex anchored via CED-9 to the mitochondrial membrane, then that complex would contain two molecules of CED-3, apparently held in such a way that autoactivation is inhibited. We have preliminary electron microscopy data showing that the negatively stained CED-4/CED-9 complex is compact (100–120 Å in diameter). Based on the molecular dimensions of APAF-1, this suggests a side-by-side arrangement of the CED-4 protomers in the heterotetramer, although no information is available on the details. In a recent paper by Chao *et al.*,[32] it was elegantly demonstrated that dimerisation of caspase-9 alone is not sufficient for full activity (compared to APAF-1-activated caspase-9). Instead, an induced conformational

change may be more important. Thus, even a head-to-head or parallel alignment (i.e. with the CED-4 CARD's aligned) may not suffice to activate CED-3 without the stimulus of EGL-1, and the resulting reorganisation of CED-4/CED-3.

We postulate an active role for CED-3 in controlling the oligomerisation of CED-4, because in its absence, CED-4 forms insoluble aggregates on release from CED-9. Future structural studies based on the results we have described should provide further insight into the molecular mechanism of this activation process.

Materials and Methods

Plasmid construction

The CED-4/CED-9 complex was coexpressed using the pET DUET-1 dual expression vector (Novagen). The wild-type or mutant *ced-4S* cDNA's were subcloned into the first multiple cloning site such that an N-terminal hexahistidine tag was added to the protein, while the wild-type or mutant FLAG-tagged *ced-9* cDNA's were subcloned into the second multiple cloning site. Hexahistidine-tagged CED-9 (amino acids 68–251) was produced using the pET 15b vector (Novagen). Mutagenesis of both CED-4 and CED-9 was performed using the method of Kunkel *et al*.[33] All constructs were confirmed by bidirectional automated DNA sequencing.

Protein expression and purification

Proteins were expressed in BL-21(DE3) pLysS cells. For the CED-4/CED-9 coexpression, cells were grown from an overnight culture to an OD_{600} of 0.6–0.8 at 37°C. Expression of proteins was then induced with 500 μM isopropyl-β-D-thiogalactopyranoside for 5 h at 25°C after which cells were pelleted and stored at −80°C until required. Uncomplexed CED-9 was expressed by induction at 37°C for 3 h.

To purify the proteins, cell pellets were thawed and homogenised using an Avestin EmulsiFlex homogeniser in lysis buffer (20 mM Tris-HCl, pH 8.0, 150 mM NaCl, 10 mM 2-mercaptoethanol: TBS/2ME). Following centrifugation to remove cell debris, the supernatant was filtered and then pumped onto a 1 ml Hi-Trap (Amersham Biosciences) chelating column charged with nickel. After washing the column with lysis buffer containing 20 mM imidazole, the protein was eluted with lysis buffer containing 250 mM imidazole. The eluate was then further purified by gel-filtration chromatography on a Superdex 200 16/60 column (Amersham) equilibrated and run in lysis buffer at 1 ml/min.

SDS-PAGE and Western blot analysis

Proteins were boiled in Laemmli sample buffer for 3 min prior to electrophoresis on precast 4–20% polyacrylamide gradient gels (Invitrogen). Gels were either stained directly in a Coomasie Brilliant Blue solution or proteins transferred to PVDF membranes for Western blot analysis. Membranes were probed using either anti-hexahistidine (Santa Cruz Biotechnology) or anti-FLAG M2 antibodies (Sigma) followed by anti-rabbit or anti-mouse horseradish peroxidase-conjugated secondary antibodies. Proteins were then visualised by enhanced chemiluminescence (Amersham Biosciences).

CED-4/CED-9 complex dissociation assays

Studies on the dissociation of the CED-4/CED-9 complex were performed by incubation of 50 μg of protein (0.5 mg/ml) with a two-fold molar excess of synthetic BH3 domain peptide (supplied by Mimotopes) in a total volume of 200 μl for 1 h at room temperature. The reaction mixture was then centrifuged for 5 min at 13 000 rpm in a bench-top microfuge prior to chromatography on a Superose 6 10/30 column equilibrated and run in TBS/2ME at 0.5 ml/min.

Isothermal titration microcalorimetry

Isothermal titration microcalorimetry (ITC) studies were performed using a MicroCal VP-ITC instrument. Proteins were diluted to 15 μM in TBS/2ME and peptides (prepared in the same buffer from 2 mM stocks) were titrated from a 120 μM solution. All experiments were performed at 25°C. Data analysis was performed using the MicroCal Origin software.

Analytical ultracentrifugation

Sedimentation experiments were conducted in a Beckman model XL-A analytical ultracentrifuge at a temperature of 20°C. Samples dissolved in 20 mM Tris, 150 mM NaCl, 1 mM DTT, pH 8.0 were loaded into a conventional double sector quartz cell and mounted in a Beckman 4-hole An-60 Ti rotor. For sedimentation velocity experiments, 380 μl of sample (1.0 mg/ml) and 400 μl of reference solution were centrifuged at a rotor speed of 40 000 rpm, and the data were collected at a single wavelength (280 nm) in continuous mode, using a time interval of 300 s and a step-size of 0.003 cm without averaging. For sedimentation equilibrium experiments, 100 μl of sample (1.0 mg/ml) and 120 μl of reference were employed and the data were collected at a wavelength of 290 nm, rotor velocity of 10 000 or 16 000 rpm, using a stepsize of 0.001 cm with 10 averages until sedimentation equilibrium was attained ($\sim$24 h). To estimate the signal due to nonsedimenting contaminants, high-speed depletion was performed at 40 000 rpm for 5 h following sedimentation equilibrium, and the resulting baseline offset (*E*) was calculated by averaging the absorbance over a radial range of 0.1 cm in the plateau region adjacent to the sample meniscus. For all samples, the values for *E* represented $<$ 5% of the initial absorbance. Solvent density (1.005 g/ml at 20°C) and viscosity (1.021 cp), as well as estimates of the partial specific volume (0.734 ml/g) and hydration (0.402 g/g) of the CED-4/CED-9ΔNΔC complex were computed using the program SEDNTERP.[34] Sedimentation velocity data at multiple time points were fitted to either a noninteracting discrete species model of up to three components or a continuous size-distribution model[35] using the program SEDFIT, which is available at www.analyticalultracentrifugation.com. Sedimentation equilibrium data at multiple speeds were globally fitted to single discrete species model by employing the program SEDPHAT,[36] which is similarly available.

N-terminal amino-acid sequencing

N-terminal amino-acid sequencing was performed using a Hewlett Packard G1000A protein sequencer.

Co-immunoprecipitations

293T cells were transiently cotransfected with pcDNA3 vectors encoding HA-tagged CED-4 and FLAG-tagged CED-9 and either EE-tagged-EGL-1 or EE-tagged Bim_S, both in pEF vectors. At 24 h post-transfection, CED-4/CED-9 complexes were immunoprecipitated using a mouse M2 anti-FLAG antibody (Sigma). Following SDS-PAGE, proteins were transferred onto nitrocellulose membranes and immunoblotted with either rat anti-HA 3F10 (Roche) or FLAG 9H1 antibodies.[37]

Acknowledgements

We thank Mr Marco Evangelista and Mr Jai Yu for excellent technical assistance and Mr Phil Strike at CSIRO Health Science and Nutrition for the protein sequencing. Our work is supported by the Australian NHMRC (Program Grant 257502 and an RD Wright Fellowship to WDF), Leukemia and Lymphoma Society (Specialized Center of Research 7015-02), Cancer Council Victoria (Fraser Fellowship to PMC), Sylvia and Charles Viertel Charitable Foundation, and Australian Cancer Research Foundation.

References

1. Horvitz HR (1999) Genetic control of programmed cell death in the nematode *Caenorhabditis elegans*. Cancer Res. 59 (7 Suppl): 1701s–1706s
2. Yuan JY and Horvitz HR (1990) The *Caenorhabditis elegans* genes *ced-3* and *ced-4* act autonomously to cause programmed cell death. Dev. Biol. 138: 33–41
3. Conradt B and Horvitz HR (1998) The *C. elegans* protein EGL-1 is required for programmed cell death and interacts with the Bcl-2-like protein CED-9. Cell 93: 519–529
4. Hengartner MO and Horvitz HR (1994) *C. elegans* cell survival gene *ced*-9 encodes a functional homolog of the mammalian proto-oncogene *bcl*-2. Cell 76: 665–676
5. Chen F, Hersh BM, Conradt B, Zhou Z, Riemer D, Gruenbaum Y and Horvitz HR (2000) Translocation of *C. elegans* CED-4 to nuclear membranes during programmed cell death. Science 287: 1485–1489
6. Yang X, Chang HY and Baltimore D (1998) Essential role of CED-4 oligomerization in CED-3 activation and apoptosis. Science 281: 1355–1357
7. Chinnaiyan AM, Chaudhary D, O'Rourke K, Koonin EV and Dixit VM (1997) Role of CED-4 in the activation of CED-3. Nature 388: 728–729
8. Parrish J, Metters H, Chen L and Xue D (2000) Demonstration of the *in vivo* interaction of key cell death regulators by structure-based design of second-site suppressors. Proc. Nat. Acad. Sci. USA 97: 11916–11921
9. Spector MS, Desnoyers S, Hoeppner DJ and Hengartner MO (1997) Interaction between the *C. elegans* cell-death regulators CED-9 and CED-4. Nature 385: 653–656
10. Ottilie S, Wang Y, Banks S, Chang J, Vigna NJ, Weeks S, Armstrong RC, Fritz LC and Oltersdorf T (1997) Mutational analysis of the interacting cell death regulators CED-9 and CED-4. Cell Death Differ. 4: 526–533
11. Tao W, Walke DW and Morgan JI (1999) Oligomerized Ced-4 kills budding yeast through a caspase-independent mechanism. Biochem. Biophys. Res. Commun. 260: 799–805
12. del Peso L, González VM and Núñez G (1998) *Caenorhabditis elegans* EGL-1 disrupts the interaction of CED-9 with CED- 4 and promotes CED-3 activation. J. Biol. Chem. 273: 33495–33500
13. Wu D, Wallen HD, Inohara N and Nuñez G (1997) Interaction and regulation of the *Caenorhabditis elegans* death protease CED-3 by CED-4 and CED-9. J. Biol. Chem. 272: 21449–21454
14. Yan N, Gu L, Kokel D, Chai J, Li W, Han A, Chen L, Xue D and Shi Y (2004) Structural, biochemical, and functional analyses of CED-9 recognition by the proapoptotic proteins EGL-1 and CED-4. Mol. Cell 15: 999–1006
15. del Peso L, González VM, Inohara N, Ellis RE and Núñez G (2000) Disruption of the CED-9/CED-4 complex by EGL-1 is a critical step for programmed cell death in *C. elegans*. J. Biol. Chem. 275: 27205–27211
16. Woo JS, Jung JS, Ha NC, Shin J, Kim KH, Lee W and Oh BH (2003) Unique structural features of a BCL-2 family protein CED-9 and bio physical characterization of CED-9/EGL-1 interactions. Cell Death Differ. 10: 1310–1319
17. Muchmore SW, Sattler M, Liang H, Meadows RP, Harlan JE, Yoon HS, Nettesheim D, Chang BS, Thompson CB, Wong S-L, Ng S-C and Fesik SW (1996) X-ray and NMR structure of human Bcl-x_L, an inhibitor of programmed cell death. Nature 381: 335–341
18. Petros AM, Medek A, Nettesheim DG, Kim DH, Yoon HS, Swift K, Matayoshi ED, Oltersdorf T and Fesik SW (2001) Solution structure of the antiapoptotic protein bcl-2. Proc. Nat. Acad. Sci. USA 98: 3012–3017
19. Liu X, Dai S, Zhu Y, Marrack P and Kappler JW (2003) The structure of a Bcl-x_L/Bim fragment complex: Implications for Bim function. Immunity 19: 341–352
20. Petros AM, Nettseheim DG, Wang Y, Olejniczak ET, Meadows RP, Mack J, Swift K, Matayoshi ED, Zhang H, Thompson CB and Fesik SW (2000) Rationale for Bcl-x_L/Bad peptide complex formation from structure, mutagenesis, and biophysical studies. Protein Sci. 9: 2528–2534
21. Sattler M, Liang H, Nettesheim D, Meadows RP, Harlan JE, Eberstadt M, Yoon HS, Shuker SB, Chang BS, Minn AJ, Thompson CB and Fesik SW (1997) Structure of Bcl-x_L-Bak peptide complex: recognition between regulators of apoptosis. Science 275: 983–986
22. Hengartner MO and Horvitz HR (1994) Activation of *C. elegans* cell death protein CED-9 by an amino-acid substitution in a domain conserved in Bcl-2. Nature 369: 318–320
23. Riedl SJ, Li W, Chao Y, Schwarzenbacher R and Shi Y (2005) Structure of the apoptotic protease-activating factor 1 bound to ADP. Nature 434: 926–933
24. Seiffert BM, Vier J and Hacker G (2002) Subcellular localization, oligomerization, and ATP-binding of *Caenorhabditis elegans* CED-4. Biochem. Biophys. Res. Commun. 290: 359–365
25. Vediyappan G, Bikandi J, Braley R and Chaffin WL (2000) Cell surface proteins of *Candida albicans*: preparation of extracts and improved detection of proteins. Electrophoresis 21: 956–961
26. Perugini MA, Schuck P and Howlett GJ (2000) Self-association of human apolipoprotein E3 and E4 in the presence and absence of phospholipid. J. Biol. Chem. 275: 36758–36765
27. Schumacher B, Schertel C, Wittenburg N, Tuck S, Mitani S, Gartner A, Conradt B and Shaham S (2005) *C. elegans* ced-13 can promote apoptosis and is induced in response to DNA damage. Cell Death Differ. 12: 153–161
28. Vaux DL, Weissman IL and Kim SK (1992) Prevention of programmed cell death in *Caenorhabditis elegans* by human bcl-2. Science 258: 1955–1957
29. Kim KJ, Kim HE, Lee KH, Han W, Yi MJ, Jeong J and Oh BH (2004) Two-promoter vector is highly efficient for overproduction of protein complexes. Protein Sci. 13: 1698–1703
30. Chen L, Willis SN, Wei A, Smith BJ, Fletcher JI, Hinds MG, Colman PM, Day CL, Adams JM and Huang DC (2005) Differential targeting of prosurvival Bcl-2 proteins by their BH3-only ligands allows complementary apoptotic function. Mol. Cell 17: 393–403
31. Chaudhary D, O'Rourke K, Chinnaiyan AM and Dixit VM (1998) The death inhibitory molecules CED-9 and CED-4L use a common mechanism to inhibit the CED-3 death protease. J. Biol. Chem. 273: 17708–17712
32. Chao Y, Shiozaki EN, Srinivasula SM, Rigotti DJ, Fairman R and Shi Y (2005) Engineering a dimeric caspase-9: a re-evaluation of the induced proximity model for caspase activation. PloS. Biol. 3: e183
33. Kunkel TA, Bebenek K and McClary J (1991) Efficient site-directed mutagenesis using uracil-containing DNA. Methods Enzymol. 204: 125–139
34. Laue TM, Shah BD, Ridgeway TM and Pelletier SL (1992) Computer aided interpretation of analytical sedimentation data for proteins. In *Analytical Ultracentrifugation in Biochemistry and Polymer Science* Harding SE, Rowe AJ and Horton JC (eds) (Cambridge: The Royal Society of Chemistry) pp. 90–125
35. Schuck P (2000) Size-distribution analysis of macromolecules by sedimentation velocity ultracentrifugation and lamm equation modeling. Biophys. J. 78: 1606–1619
36. Vistica J, Dam J, Balbo A, Yikilmaz E, Mariuzza RA, Rouault TA and Schuck P (2004) Sedimentation equilibrium analysis of protein interactions with global implicit mass conservation constraints and systematic noise decomposition. Anal. Biochem. 326: 234–256
37. Wilson-Annan J, O'Reilly LA, Crawford SA, Hausmann G, Beaumont JG, Parma LP, Chen L, Lackmann M, Lithgow T, Hinds MG, Day CL, Adams JM and Huang DC (2003) Proapoptotic BH3-only proteins trigger membrane integration of prosurvival Bcl-w and neutralize its activity. J. Cell Biol. 162: 877–887

Supplementary Information accompanies the paper on Cell Death and Diffrentiation website (http://www.nature.com/cdd).